ARTICLE

OBC
www.rsc.org/obc

Xanthenol clathrates: structure, thermal stability, guest exchange and kinetics of desolvation

Ayesha Jacobs,*[a] Luigi R. Nassimbeni,[a] Hong Su[b] and Benjamin Taljaard[c]

[a] *Department of Interdisciplinary Maths and Science Studies, Faculty of Applied Sciences, Cape Town Campus, Cape Peninsula University of Technology, P.O. Box 652, Cape Town, 8000, South Africa. E-mail: jacobsa@cput.ac.za; Fax: 27 21 460 3854; Tel: 27 21 460 3167*

[b] *Department of Chemistry, University of Cape Town, Rondebosch, 7701, South Africa*

[c] *Department of Chemistry, Nelson Mandela Metropolitan University, 6031, South Africa*

Received 26th October 2004, Accepted 11th February 2005
First published as an Advance Article on the web 4th March 2005

A series of clathrates comprising the xanthenol host, 9-(4-methoxyphenyl)-9*H*-xanthen-9-ol, with a variety of aromatic guests displays similar structures in the space group $P(-1)$. We have elucidated the structures of the inclusion compounds H·$\frac{1}{2}$G, where H is 9-(4-methoxyphenyl)-9*H*-xanthen-9-ol and G is benzene, *o*-, *m*- and *p*-xylene. The structures are isostructural with respect to the host and display consistent (Host)–OH $\cdots$ O–(Host) hydrogen bonding. The guests lie on a centre of inversion and with the exception of the symmetrical guests, benzene and *p*-xylene, are disordered. An interesting case arises with *m*-xylene, which is ordered at low temperature (113 K) with both the host and guest molecules in general positions. At a higher temperature (283 K) the inclusion compound with *m*-xylene fits the series. We have correlated the structures with their thermal stabilities, guest exchange and kinetics of desolvation.

Introduction

The field of inclusion chemistry has grown dramatically in recent years, and most of the work has been directed at the syntheses of novel host compounds with specific properties. The stoichiometry and topology of an inclusion compound in the solid state depends on the extent of molecular recognition which occurs between the host and guest molecules, and the resultant structure can, in principle, explain its reactivity and stability. Several books, monographs and reviews are available[1–4] which describe the properties and uses of inclusion compounds, and which form an important aspect of crystal engineering. The host 9-(4-methoxyphenyl)-9*H*-xanthen-9-ol, **H**, is an organic host compound which conforms to Weber's rules for host design.[5] in that it is bulky, rigid, and has an hydroxyl moiety that acts as a hydrogen-bond donor, as well as an ether oxygen which is a potential hydrogen bond acceptor. In this work we describe the structures of its inclusion compounds with benzene and the isomers of xylene, as well as their stabilities, guest exchange and kinetics of desolvation. The atomic numbering of the inclusion compounds is shown in Scheme 1.

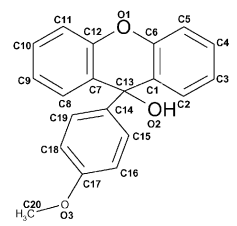

9-(4-methoxy-phenyl)-9H-xanthen-9-ol (H)

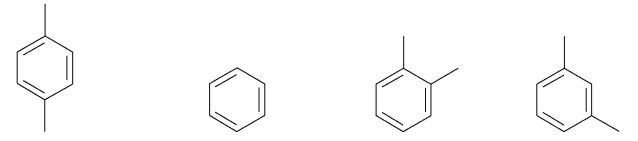

1a = **H**•½*p*-xylene; 1b, *2* = **H**•½benzene; *3* = **H**•½*o*-xylene; *4* = **H**•½*m*-xylene(283K); *5* = **H**•½*m*-xylene(113K)

Scheme 1

Experimental

Structure analysis

Crystals of all the inclusion compounds† were obtained by slow evaporation of solutions of the host dissolved in excess liquid guest. Thermogravimetry (TG) was employed to determine the host : guest ratios. Details of the crystal data, intensity data collection and refinement are given in Table 1. Cell dimensions were established from the intensity data measured on a Kappa CCD diffractometer using graphite-monochromated MoK_α radiation. The strategy for the data collection was evaluated using COLLECT software[6] and for all structures the intensity data were collected by the standard phi scan and omega scan techniques and were scaled and reduced using the program DENZO-SMN.[7] The structures were solved by direct methods using SHELX-86[8] and refined by full-matrix least-squares with SHELX-97,[9] refining on F^2. The program X-Seed[10] was used as a graphical interface. In each of the structures the positions of all the non-hydrogen host atoms were obtained by direct methods and all guest non-hydrogen atoms were located in difference electron density maps. The host hydroxyl hydrogens were located in the difference electron density maps and refined isotropically with simple bond length restraints based on the relationship between O–H and O $\cdots$ O distances[11]. For structures **3**, H·$\frac{1}{2}$*o*-xylene, and **4**, H·$\frac{1}{2}$*m*-xylene at 283 K, the guests are disordered. In particular, C1G and C2G of the *o*-xylene guest and C1G, C3G, C5G and C6G of the *m*-xylene guest were placed with a site occupancy factor of $\frac{1}{2}$. Residual electron density minimum and maximum peaks of -1.089 and 1.741 e Å^{-3} found near the *o*-xylene guest could not be modelled successfully. For structures **1(a, b)**, **2** and **5** the non-hydrogen atoms of the guests were refined anisotropically and their hydrogens were placed with geometric constraints and refined with isotropic temperature factors.

Thermal analysis and kinetics of desolvation

Thermogravimetry (TG) was performed on a Perkin-Elmer Pyris 6 TGA and differential scanning calorimetry (DSC) was carried

† CCDC reference numbers 239532–239535 and 253840–253843. See http://www.rsc.org/suppdata/ob/b4/b416331a/ for crystallographic data in .cif or other electronic format.

DOI: 10.1039/b416331a

Table 1 Crystal data

	1a	1b	2	3	4	5	%|Δ|
Time of exposure	0	52 h	N/A	N/A	N/A	N/A	N/A
Guest	*p*-xylene	Benzene	Benzene	*o*-Xylene	*m*-Xylene	*m*-Xylene	N/A
Compound	$\mathbf{H}^{a}\cdot\frac{1}{2}C_8H_{10}$	$\mathbf{H}^{a}\cdot\frac{1}{2}C_6H_6$	$\mathbf{H}^{a}\cdot\frac{1}{2}C_6H_6$	$\mathbf{H}^{a}\cdot\frac{1}{2}C_8H_{10}$	$\mathbf{H}^{a}\cdot\frac{1}{2}C_8H_{10}$	$2\mathbf{H}^{a}\cdot C_8H_{10}$	N/A
M/g mol^{-1}	357.41	343.38	343.38	357.41	357.41	714.82	N/A
T/*K*	113(2)	113(2)	113(2)	113(2)	283	113(2)	N/A
Crystal system	Triclinic	Triclinic	Triclinic	Triclinic	Triclinic	Triclinic	N/A
Space group	$P(-1)$	$P(-1)$	$P(-1)$	$P(-1)$	$P(-1)$	$P(-1)$	N/A
a/Å	8.3773(2)	8.3763(1)	8.3757(1)	8.3654(1)	8.4902(1)	8.4150(2)	0.02
b/Å	9.1657(3)	9.0965(2)	9.1004(1)	9.0652(1)	9.1923(1)	18.2852(3)	0.72
c/Å	12.7261(4)	12.6943(3)	12.6928(2)	12.8730(3)	12.9946(2)	12.7741(4)	0.26
α/°	94.810(1)	97.485(1)	97.541(1)	96.696(1)	95.620(1)	95.637(1)	2.80
β/°	96.374(1)	104.164(1)	104.053(1)	94.048(1)	94.840(1)	94.919(1)	7.38
γ/°	108.948(1)	109.388(1)	109.405(1)	109.717(1)	109.660(1)	109.717(1)	0.42
V/Å^3	910.99(5)	860.68(3)	861.14(2)	906.38(3)	942.97(2)	1826.47(8)	5.79
Z	2	2	2	2	2	2	N/A
μ/mm^{-1}	0.085	0.087	0.087	0.085	0.082	0.085	N/A
F(000)	378	362	362	378	378	756	N/A
Unique Reflections	3932	3760	3932	4095	4106	7957	N/A
ρ_{calc}/g cm^{-3}	1.303	1.325	1.324	1.310	1.259	1.300	N/A
Final R indices [$I > 2\sigma(I)$]	$R_1 = 0.0567$, $wR_2 = 0.1596$	$R_1 = 0.0510$, $wR_2 = 0.1457$	$R_1 = 0.0396$, $wR_2 = 0.1032$	$R_1 = 0.0904$, $wR_2 = 0.2273$	$R_1 = 0.0746$, $wR_2 = 0.2286$	$R_1 = 0.0485$, $wR_2 = 0.1133$	N/A
R indices (all data)	$R_1 = 0.0879$, $wR_2 = 0.2074$	$R_1 = 0.0890$, $wR_2 = 0.2044$	$R_1 = 0.0486$, $wR_2 = 0.1087$	$R_1 = 0.0990$, $wR_2 = 0.2341$	$R_1 = 0.0904$, $wR_2 = 0.2463$	$R_1 = 0.0914$, $wR_2 = 0.1300$	N/A
Largest difference peak and hole/e Å^{-3}	0.870 and −1.037	0.907 and −1.047	0.297 and −0.274	1.741 and −1.089	0.669 and −0.524	0.246 and −0.253	N/A
Mosaic spread/°	0.719(2)	0.878(2)	0.765(2)	0.699(2)	0.674(1)	0.648(2)	N/A

[a] $C_{20}H_{16}O_3$. **1b** obtained from single crystal **1a** exposed to benzene vapour for 52 hours. %|Δ| − % absolute difference in cell parameter P:100|***P*1a** − ***P*2**|/***P*2**

out on a Perkin-Elmer PC7-Series system. The TG and DSC experiments were performed over the temperature range 303 K to 473 K at a heating rate of 10 K min^{-1} with a purge of dry nitrogen flowing at 30 ml min^{-1}. The samples were crushed, blotted dry and placed in open ceramic pans for TG and in crimped but vented pans for DSC. Data for isothermal kinetics were obtained from TG at selected temperatures.

Guest exchange

We carried out the guest-exchange reaction

$$\boldsymbol{H}\cdot\tfrac{1}{2}p\text{-xylene (s)} + \text{benzene (g)} \rightarrow \boldsymbol{H}\cdot\tfrac{1}{2}\text{benzene (s)}$$

by exposing a single crystal of the *p*-xylene clathrate (0.22 × 0.30 × 0.42 mm) to benzene vapour in a closed desiccator at 25 °C. After 15 hours of exposure the single crystal remained transparent and exhibited uniform extinction between crossed polarisers. We analysed a batch of similar-sized crystals of the *p*-xylene clathrate exposed to benzene for the same period (15 hours) and measured the relative amounts of the two guests by gas chromatography, which yielded the result of $X_{p\text{-xylene}} = 0.52$ and $X_{\text{benzene}} = 0.48$, showing that the extent of reaction was approximately half after this time. The reverse reaction carried out by exposing crystals of $\mathbf{H}\cdot\frac{1}{2}$benzene to *p*-xylene, did not occur, despite the crystal being exposed to *p*-xylene vapour at 25 °C for 5 days. We note that *p*-xylene has a lower vapour pressure than benzene and therefore the attempted reverse reaction was carried out over a longer time period.

Results and discussion

Thermogravimetry confirmed that the host : guest ratio for all the compounds was 1 : $\frac{1}{2}$. For structures **1a** to **4** the space group is $P(-1)$ and two host molecules form a centrosymmetric dimer about the centre of inversion at the Wyckoff position *h*, while the guest lies on a centre of inversion at the Wyckoff position *a*. This is displayed in Fig. 1, which shows that the host dimer is stabilised by (Host)–OH $\cdots$ O–(Host) hydrogen bonds. In the case of $\mathbf{H}\cdot\frac{1}{2}o$-xylene, **3**, and $\mathbf{H}\cdot\frac{1}{2}m$-xylene at room temperature, **4**, the guests are disordered.

Fig. 1 Typical xanthenol dimer structure with the aromatic guest at the origin of the triclinic cell.

For structure **1a**, the *p*-xylene guest lies in channels running parallel to [010], and these facilitated the single crystal–single crystal exchange reaction with benzene vapour at least in the initial stages of the reaction. The open channels of **1a** are shown in Fig. 2. The structure with the benzene guest, **H**·$\frac{1}{2}$benzene, **2**, is similar to **1a**, and again displays the host dimer with the benzene located on the centre of symmetry at the Wyckoff position *a*. However the channels in which the benzene guests are located are strongly constricted so that the benzene molecules are effectively situated in cavities, making **H**·$\frac{1}{2}$benzene a true clathrate structure. We note that the conformation of the hydrogen bonded host dimer is very similar in structures **1a** and **2**, but their packing is sufficiently different to close the channels in **H**·$\frac{1}{2}$*p*-xylene to cavities in **H**·$\frac{1}{2}$benzene. This is illustrated in Fig. 3a and 3b. The crystal obtained by exposing the *p*-xylene structure to benzene vapour for 52 hours at 25 °C yielded only the benzene structure (**1b**), showing the exchange reaction to be complete. We note that although the unit cells of structures **1a** and **2** are similar, the percentage differences in some parameters are sufficiently large to yield distinctive diffraction patterns which could not be indexed in terms of a single unit cell. We regard these structures as quasi-isomorphous, and sufficiently similar to display a single crystal–single crystal exchange reaction.

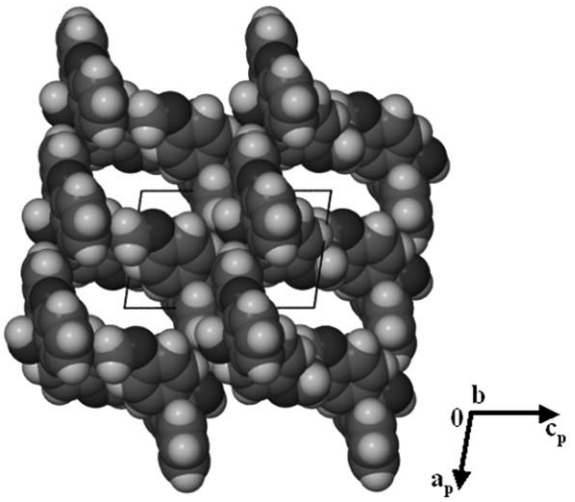

Fig. 2 Space-filling projection of **1a** along [010] with guest *p*-xylene omitted, showing the open channels.

For structures **3**, **H**·$\frac{1}{2}$*o*-xylene, and **4**, **H**·$\frac{1}{2}$*m*-xylene at 283 K, the guest molecules are disordered and situated on a centre of symmetry at Wyckoff position *a*. Both the *o*-xylene and the *m*-xylene guests were refined isotropically with the hydrogen atoms omitted from the final model. We noted that upon cooling the *m*-xylene compound from 283 K to 113 K, the crystal underwent a transformation yielding a new cell in which the *b* parameter effectively doubled, while the other parameters remained essentially unchanged. The notable difference between structures **4** and **5** is that since the cell volume is doubled in the low temperature structure, there are four hosts and two *m*-xylene guests in the unit cell. The *m*-xylene guest now lies in a general position and is ordered. The topology of structures **3**, **4** and **5** are similar in that they exhibit channels parallel to [010], in which the guest xylenes are located.

The thermal analysis results are summarised in Table 2. Overall there is good agreement between the experimental and calculated host : guest ratios, with 1 : $\frac{1}{2}$ the host : guest ratio for all compounds. The DSC curves for the benzene, *m*-xylene and *p*-xylene compounds show two distinct endotherms corresponding to loss of guest and the host melt. A single endotherm is observed for the *o*-xylene compound which we interpret as the dissolution of the host in the ensuing guest. This is an unusual result as the xylene isomers have similar boiling points and one would expect their inclusion compounds to have comparable DSC's.

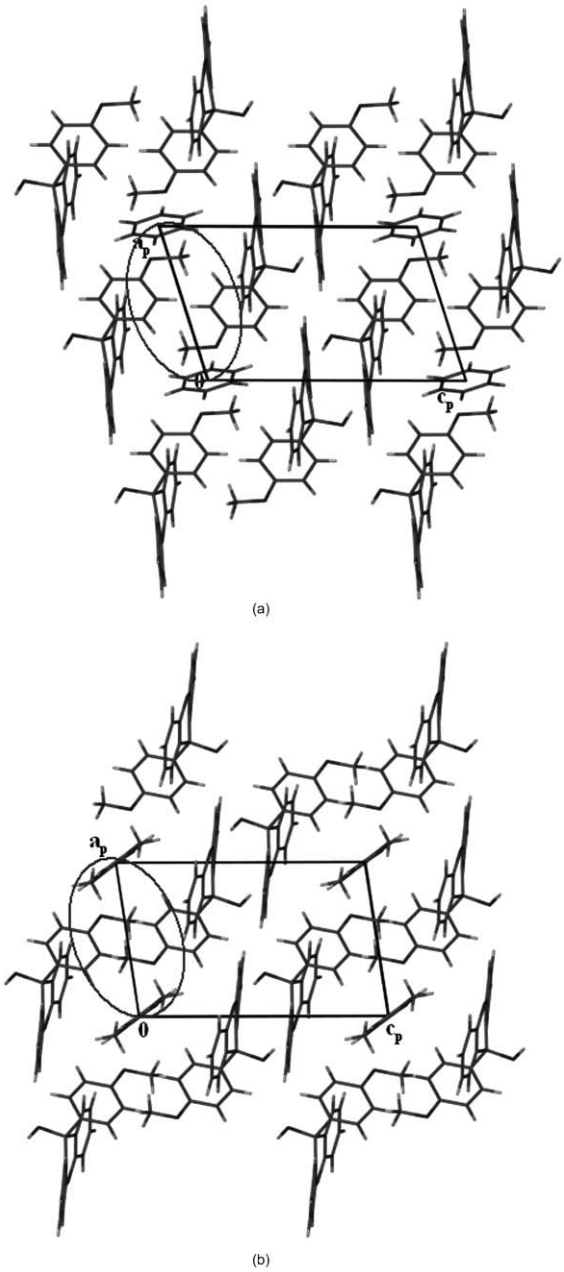

Fig. 3 Packing diagrams of (a) **2** and (b) **1a** down [010] with the encircled regions indicating the packing differences of the hydrogen bonded host dimer.

Table 2 Thermal analysis data

Inclusion compound	**1a**	**2**	**3**	**4/5**
H : G ratio	1 : $\frac{1}{2}$	1 : $\frac{1}{2}$	1 : $\frac{1}{2}$	1 : $\frac{1}{2}$
TG (calc % mass loss)	14.9	11.3	14.9	14.9
(exp % mass loss)	14.5	11.2	14.6	14.5
DSC T_{peak}/K	354.4	366.8	371.2	351.0
T_{melt}/K	393.9	392.1	—	388.0
[a] T_b/K	411	353	417	412

[a] Normal boiling point.

Kinetics of desolvation were determined for compounds **1a**, **H**·$\frac{1}{2}$*p*-xylene, and **2**, **H**·$\frac{1}{2}$benzene, by performing a series of isothermal TG experiments between 323 K and 353 K. For the *p*-xylene compound the resultant mass–time curves were sigmoidal and fitted the Avrami–Erofeev rate law (A4):

$$[-\ln(1-\alpha)]^{\frac{1}{4}} = kt$$

where α is the extent of the reaction and k is the rate constant.[12] The Arrhenius constants yielded values of ln $A = 30.8$ and the activation energy, Ea = 93.5 kJ mol^{-1}. The benzene compound desolvated in a two step manner which is non-stoichiometric. Both steps followed the deceleratory first order rate law (F1): $-\ln(1-\alpha) = kt$. For this reaction the Arrhenius constants were ln $A = 21.1$, Ea = 63.9 kJ mol^{-1} (first desolvation step) and ln $A = 40.1$, Ea = 120 kJ mol^{-1} (second desolvation step). The corresponding Arrhenius plots for both compounds are shown in Fig. 4a–4c.

When comparing the kinetics of desolvation of the *p*-xylene compound with the first desolvation step of the benzene compound, we note that the former has a larger activation energy. This is counter-intuitive because the *p*-xylene molecules are located in channels and should desorb more easily than the benzene guests which are trapped in cavities. However we note that the isokinetic effect, which occurs in the decomposition of solids, requires a compensation behaviour such that a decrease in rate due to an increase in activation energy, is offset by a larger magnitude in ln A.[13] Thus at 343 K, the rate constants for the *p*-xylene and benzene desolvations are $k = 0.138$ min^{-1} and 0.284 min^{-1}. The latter desolvation is therefore faster, which we attribute to the higher vapour pressure of benzene (549.5 torr) over *p*-xylene (78.7 torr) at 343 K.[14]

We have calculated the lattice energies of the crystal structures by the method of atom–atom potentials using the OPIX program.[15] The functional form for the i–j atom–atom potential used is

$$E_{ij} = A \cdot \exp(-BR_{ij}) - C/R_{ij}^{6}$$

where R_{ij} is the interatomic distance and the coefficients A, B and C have been carefully normalised against the known sublimation energies of selected organic compounds. We used the crystal structure data collected at the lowest temperature (113 K) for each inclusion compound. We obtained the following lattice energy values in kJ mol^{-1} per two host and one guest pair (**2H·G**): **H**·$\frac{1}{2}$benzene: −390.4; **H**·$\frac{1}{2}$*p*-xylene: −402.6; **H**·$\frac{1}{2}$*m*-xylene: −401.2; **H**·$\frac{1}{2}$*o*-xylene: −402.3. We are aware that comparison of lattice energies is only valid between structures with the same number of atoms. Therefore we normalized the lattice energy of **H**·$\frac{1}{2}$benzene according to its molecular weight in relation to those of the xylene compounds, and we obtained −405.2 kJ mol^{-1}. We note that the lattice energies of all the four inclusion compounds are very close which explains the ability of this particular host to include a wide variety of aromatic compounds.

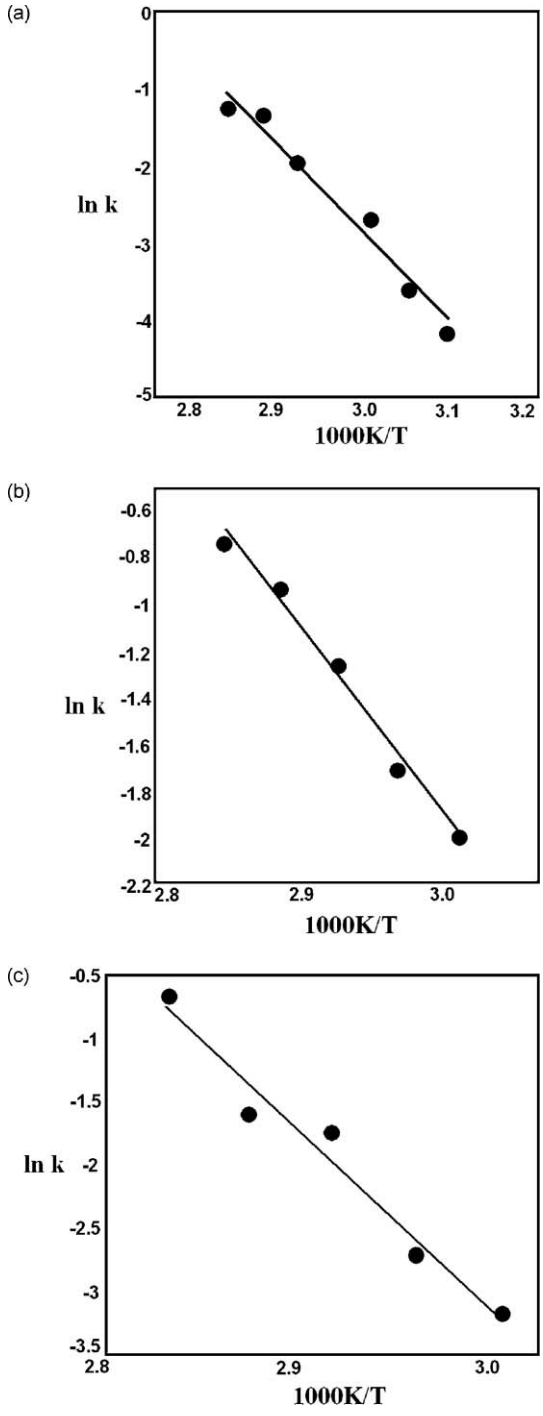

Fig. 4 Arrhenius plots for compounds (a) **1a**, (b) **2** (first desolvation step) and (c) **2** (second desolvation step).

Acknowledgements

The authors thank the National Research Foundation (Pretoria) for Research Grants.

References

1 Comprehensive Supramolecular Chemistry, in *Solid State Supramolecular Chemistry: Crystal Engineering*, ed. D. D. MacNicol, F. Toda and R. Bishop, Pergamon, Oxford, vol. 6, 1996.
2 G. R. Desiraju, *Crystal Engineering*, Elsevier, Amsterdam, 1989.
3 *Crystal Engineering: From Molecules and Crystals to Materials*, ed. D. Braga, F. Grepioni and A. G. Orpen, Kluwer Academic Press, Dordrecht, 1999.
4 L. R. Nassimbeni, *Acc. Chem. Res.*, 2003, **36**, 631.
5 E. Weber, *Inclusion Compounds*, ed. J. L. Atwood, J. E. D. Davies and D. D. MacNicol, Oxford University Press, Oxford, 1991, ch. 5.
6 *COLLECT, data collection software*, Nonius, Delft, The Netherlands, 1998.
7 Z. Otwinowski and W. Minor, in *Methods in Enzymology, Macromolecular Crystallography*, ed. C. W. Carter and R. M. Sweet, Academic Press, New York, 1997, part A, vol. 276, pp. 307–326.
8 G. M. Sheldrick, in *Crystallographic Computing*, ed. G. M. Sheldrick, C. Kruger and P. Goddard, Oxford University Press, Oxford, 1985, vol. 3, pp. 175.
9 G. M. Sheldrick, *SHELX-97, Program for Crystal Structure Deteremination*, University of Göttingen, Germany, 1997.
10 L. J. Barbour, *X-Seed, Graphical Interface for SHELX Program*, University of Missouri, Columbia, USA, 1999.
11 I. Olovsson and P. Jönsson, *The Hydrogen Bond-Structure and Spectroscopy*, ed. P. Schuster, G. Zundel and C. Sardify, North Holland Publishing Company, USA, 1975.
12 M. E. Brown, *Introduction to Thermal Analysis*, Chapman and Hall, New York, ch. 13.
13 A. K. Galwey and M. E. Brown, Handbook of Thermal Analysis and Calorimetry, ed. M. E. Brown, vol 1, *Principles and Practice*, Elsevier, Amsterdam, 1998, ch. 3.
14 J. A. Dean, *Lange's Handbook of Chemistry*, 14th edn, McGraw-Hill Inc., 1992.
15 A. Gavezzotti, OPIX, *A computer program package for the calculation of intermolecular interactions and crystal energies*, University of Milano, 2003.